Effects of Edge Oxidation on the Structural, Electronic, and Magnetic Properties of Zigzag Boron Nitride Nanoribbons

Supporting Information

Dana Krepel and Oded Hod

Department of Chemical Physics, School of Chemistry, The Raymond and Beverly Sackler Faculty of Exact Sciences, Tel Aviv University, Tel Aviv 69978, Israel

Effects of choice of basis set on the calculated relative stability and bandgaps

In order to evaluate the convergence of our results with respect to the choice of basis set we repeated some relative stability and field dependent bandgap calculations using the 3-21G and cc-pVDZ basis sets and compared the results to those obtained with the double-zeta polarized 6-31G** basis set used throughout the calculations presented in the main text. In panel (a) of Fig. S1 we compare the relative stabilities of edge decorated 6x4 ZBNNRs (see Fig. 10 of the main text), calculated with the HSE functional approximation via Eq. 1 of the main text, using the 6-31G** and cc-pVDZ basis sets. As can be seen, the largest difference is obtained for the hydrogen terminated ZBNNRs, with difference of ~5% between the results obtained using the two basis sets, thus indicating the convergence our stability calculations using the 6-31G** basis set.

Further calculations have been performed to evaluate the convergence of the electronic structure calculations. In panel (b) of Fig. S1 we present the α spin bandgap variations as a function of external electric field intensity (see Fig. 7 of the main text) calculated for the hydrogen terminated 6x4 ZBNNRs with the HSE functional approximation and using the 3-21G, 6-31G**, and cc-pVDZ basis sets. The field-free calculated bandgap are found to be converged to within 2% as indicated from the difference between the 6-31G** and cc-pVDZ results. Somewhat smaller differences (0.7%) were found between the results obtained using the 3-21G and 6-31G** basis sets. In the presence of an external electric field, the calculated bandgap does become more sensitive to the choice of basis-set, however the overall difference between the 6-31G** and cc-pVDZ values do not exceed 20% and the general trends are the same. Hence, we conclude that our choice of the 6-31G** is valid for all practical purposes.
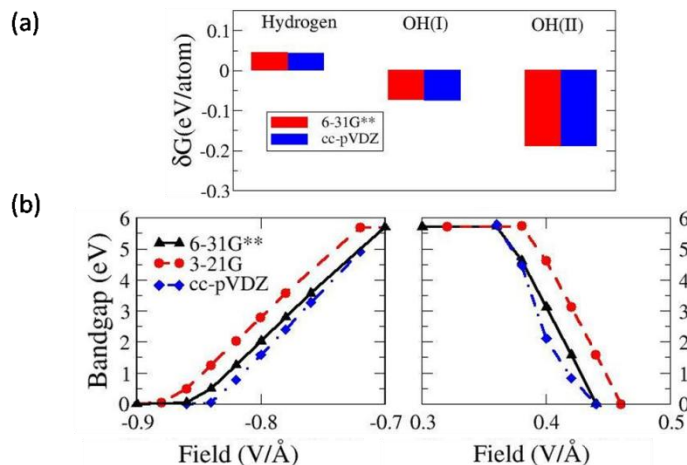
Fig. S1: Basis set convergence for the 6x4 ZBNNR. (a) Relative stabilities of the H, OH(I), and OH(II) oxidation schemes (see Fig. 1 of the main text) as obtained via Eq. (1) of the main text using the HSE functional approximation and the 6-31G** (red bars) and cc-pVDZ (blue bars) basis sets. (b) α spin bandgaps of the hydrogenated system as a function of the field intensity and direction calculated using the HSE functional approximation and the 3-21G (red circles), 6-31G** (black triangles), and cc-pVDZ (blue diamonds) basis sets. Negative values indicate stable structures with respect to the constituents.

Effects of choice of functional approximation on the calculated relative stability

In Fig. 2 of the main text we have presented the relative stability of the various structures studied as calculated using the HSE functional approximation. Here, for completeness, we present similar results obtained using the LDA and PBE functionals. As can be seen in Fig. S2, similar trends are obtained using the (semi-)local functional approximations. The main difference is found in the relative stability of the triplet spin state of some adsorption schemes: for the OH(I) adsorption scheme, although the singlet spin state is found to be the most stable spin state for all functional approximations considered, the calculated stability of the triplet state is found to decrease for both the PBE and LDA functional reaching positive δG values of 0.07 eV for the and 0.09 eV for the LDA and PBE functional approximations, respectively as compared to the HSE value of -0.04 eV. In addition, it is found that for the Et(II) adsorption scheme, the triplet spin state is the most stable spin state for all functional approximations considered. However, when comparing its relative stability, while for the HSE functional a positive δG value of 0.05eV is obtained, for the LDA and PBE functional approximations negative values of -0.08 eV and -0.04 eV are calculated. It should be noted that, although the triplet state of the Et(II) scheme is found to be stable with respect to its constituents, the relative stabilities of the singlet states of both the OH(I) and OH(II) schemes are found to be more stable for all functional approximations considered.
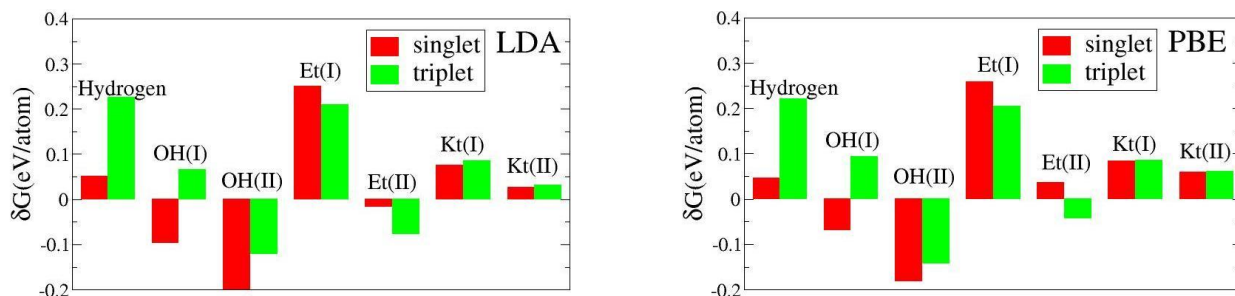
2

Figure S2: Ground state relative stabilities of the different oxidized systems studied (see Fig. 1 of the main text) obtained via Eq. (1) of the main text at the LDA/6-31G** (left panel) and PBE/6-31G** (right panel) levels of theory. Negative values indicate stable structures with respect to the constituents. Results of the singlet and triplet spin state calculations are presented in red and green bars, respectively.

Effects of choice of functional approximation on the calculated bandgaps

In Fig. 3 of the main text we have presented the bandgaps of the various structures obtained using the HSE functional approximation. Here, for completeness, we present similar results obtained using the LDA and PBE functionals. As can be seen in Fig. S3, all functionals considered present similar trends. As may be expected, the bandgaps predicted using the (semi-)local functional approximations are somewhat smaller such that for a given structure the bandgap ordering is usually $E_g(HSE)>E_g(PBE)>E_g(LDA)$. As stated in the manuscript, the Ket(II) oxidation scheme is found to be of metallic nature for both the LDA and PBE functional approximations.
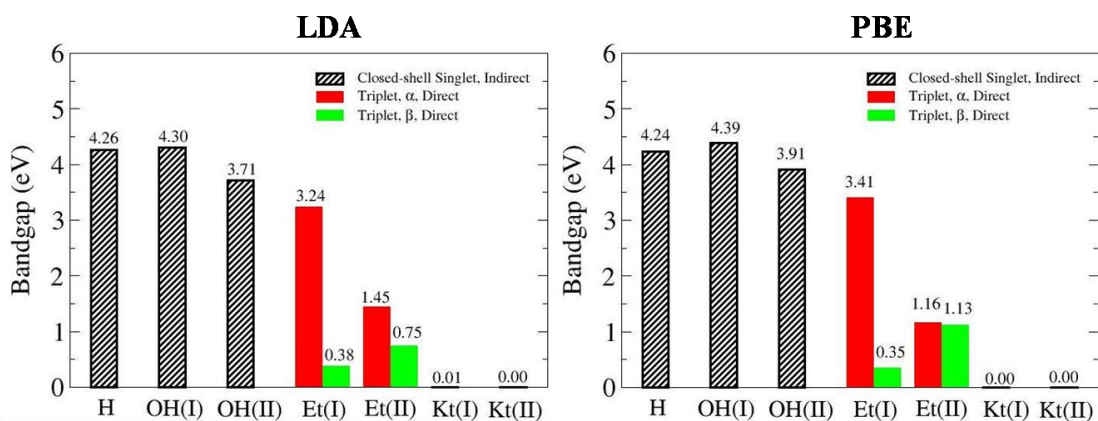

Fig. S3: Bandgaps of the various systems considered as calculated at the LDA/6-31G** (left panel) and PBE/6-31G** (right panel) levels of theory. The singlet spin state is represented by black bars whereas the triplet spin state is represented by red (α spin electrons) and green (β spin electrons) bars. Full and striped bars represent direct and indirect bandgaps, respectively.

Band-structures, FDOSs, and PDOSs of the Et(I) and Et(II) systems

In Fig. 4 of the main text we have presented the band-structures, FDOS and PDOS of the H, OH(I), OH(II) and Ket(I) oxidation schemes as calculated at the HSE/6-31G** level of theory. Here, for completeness, we present similar results for the Et(I), Et(II), and Kt(II) oxidation schemes at the same level of theory. For the Et(I) and Et(II) oxidation schemes, a similar behavior as that presented in the main text is obtained for the α spin states of both these oxidation schemes with an enhanced contribution of the N-edge to the upper valence bands including the HOCO. For the β spin states, noticeable flat bands, again associated with the N-edge, appear in the gap region. For the Kt(II) oxidation scheme, the α and β spin states are degenerate and have a narrow direct X point gap of ~0.15eV. Similar to the Kt(I) oxidation scheme, Kt(II) oxidation is found to p-dope the system by shifting the Fermi energy into the valence band. Also, the bands around the Fermi level are contributed not only from the ribbon itself, but also from the oxygen atoms at the N-edge.
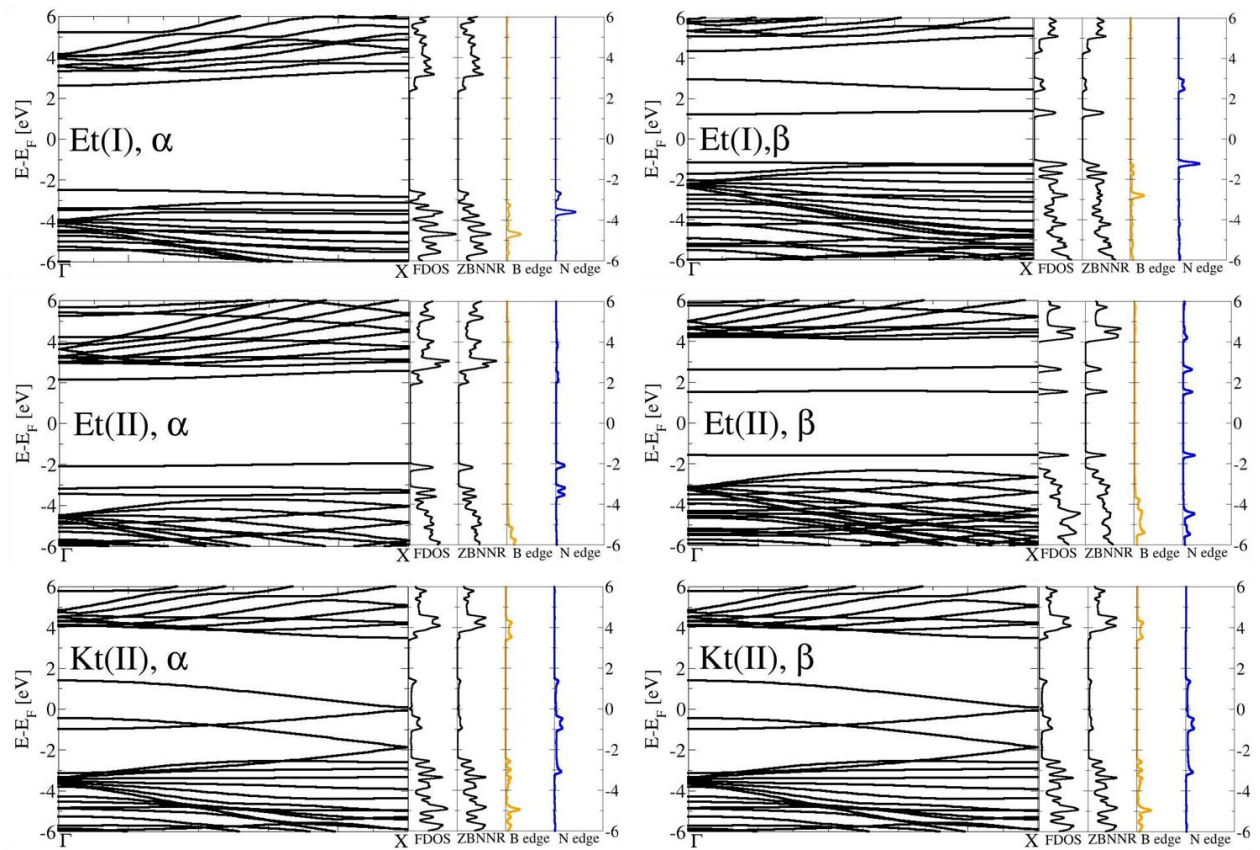

Figure S4: α (left panels) and β (right panels) spin band-structures, FDOS, and PDOS of the Et(I) (upper panels) and Et(II) (lower panels) oxidation schemes as calculated at the HSE/6-31G** level of theory. Fermi energies of all diagrams are set to zero.

Band-structures, FDOSs, and PDOSs of the OH(II) system at various electric fields

In Fig. 8 of the main text we have presented the band-structures, FDOS and PDOS of the H-terminated ZBNNRs at various external electric-field intensities as calculated at the HSE/6-31G** level of theory. Here, for completeness, we present similar results for the OH(II) oxidation scheme calculated at the same level of theory. The electronic response of both decoration schemes is similar, resulting in two (or more) energy bands originating from the field-less conduction band and penetrating the gap region with a parabolic-like dispersion relation thus considerably reducing the value of the bandgap. Moreover, the partial DOS analysis reveals that here as well these bands are associated with the central section of the ribbons and not with its edges constituents.
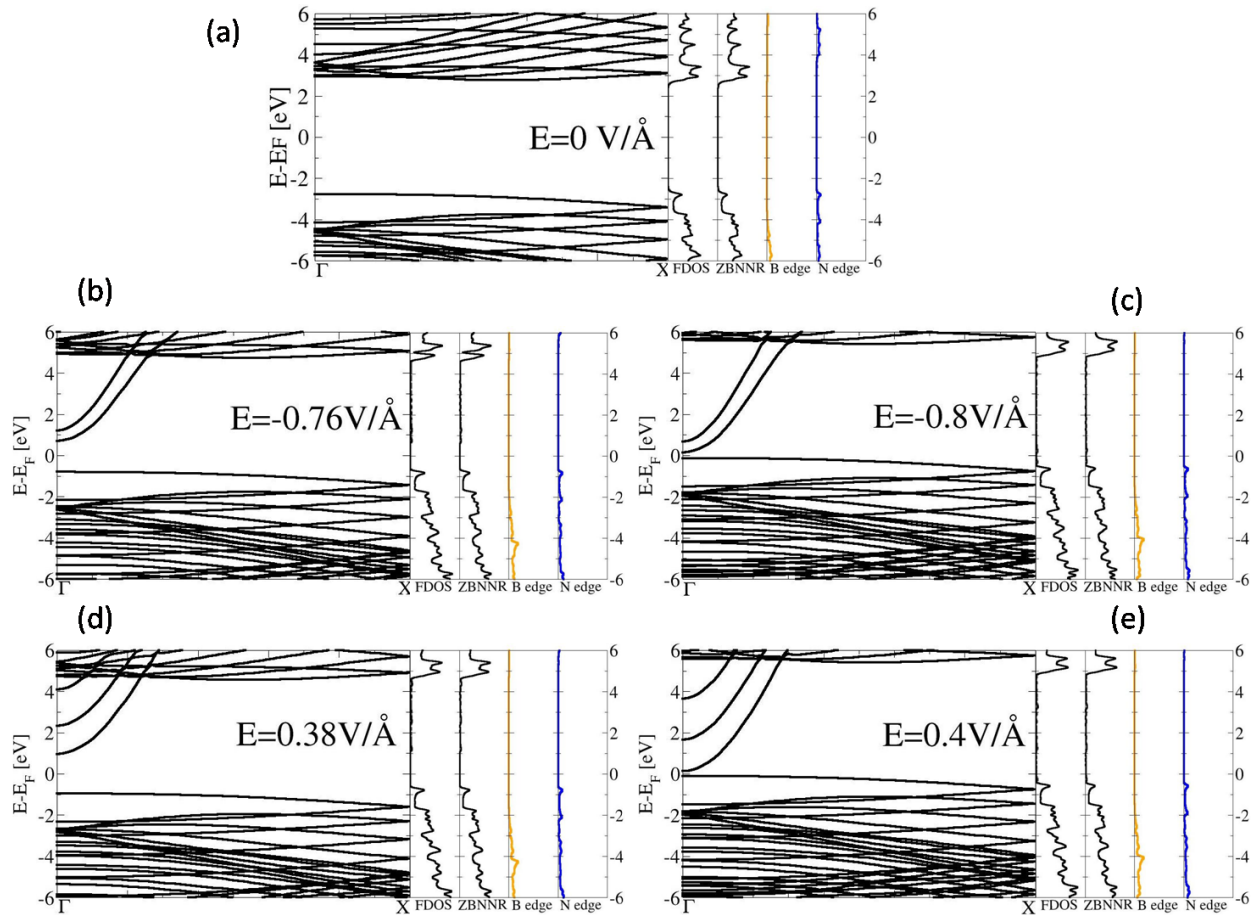

Figure S5: Band-structures, FDOS, and PDOS of the α spin state of the OH(II)-terminated ZBNNR at the following fields: (a) 0V/Å, (b) -0.76 V/Å (c) -0.8V/Å (d) +0.38V/Å, and (e) +0.4 V/Å as calculated at the HSE/6-31G** level of theory. Fermi energies of all diagrams are set to zero.